LAWRENCE
LIVERMORE
NATIONAL
LABORATORY

LLNL-CONF-404568

Advances Towards Readily Deployable Antineutrino Detectors for Reactor Monitoring and Safeguards

N. S. Bowden, A. Bernstein, S. Dazeley, J. Lund, D. Reyna, L. Sadler, R. Svoboda

June 10, 2008

Institute of Nuclear Materials Management
Nashville, TN, United States
July 13, 2008 through July 17, 2008

Advances Towards Readily Deployable Antineutrino Detectors for Reactor Monitoring and Safeguards

N. S. Bowden[a], A. Bernstein[a], S. Dazeley[a], J. Lund[b], D. Reyna[b], L. Sadler[b], R. Svoboda[a]
[a]*Lawrence Livermore National Laboratory, Livermore, CA 94550*
[b]*Sandia National Laboratories California, Livermore, CA 94550*

Abstract

Nuclear reactors have served as the neutrino source for many fundamental physics experiments. The techniques developed by these experiments make it possible to use these very weakly interacting particles for a practical purpose. The large flux of antineutrinos that leaves a reactor carries information about two quantities of interest for safeguards: the reactor power and fissile inventory. Our LLNL/SNL collaboration has demonstrated that such antineutrino based monitoring is feasible using a relatively small cubic meter scale detector at tens of meters standoff from a commercial PWR. With little or no burden on the plant operator we have been able to remotely and automatically monitor the reactor operational status (on/off), power level, and fuel burnup. Recently, we have investigated several technology paths that could allow such devices to be more readily deployed in the field. In particular, we have developed and fielded two new detectors; a low cost, non- flammable water based design; and a robust solid-state design based upon plastic scintillator. Here we will describe the tradeoffs inherent in these designs, and present results from their field deployments.

1 Introduction

Reactor safeguards regimes, such as that implemented by the International Atomic Energy Agency (IAEA) in accordance with the Non-proliferation Treaty (NPT), are designed to detect and deter illicit or suspicious uses of these facilities. In large part, reactors are safeguarded by indirect means that do not involve the direct measurement of the fissile isotopic content of the reactor, but instead rely primarily on semi-annual or annual inspections of coded tags and seals placed on fuel assemblies, and measures such as video surveillance of spent fuel cooling ponds. When direct measurements do take place, they are implemented offline, before or after fuel is introduced into the reactor. These may include the counting of fuel bundles or the checking of the enrichment of random samples of fresh or spent fuel rods. Under the IAEA regime, reactor operators are additionally required to submit periodic declarations of their fissile holdings, including the amount of plutonium generated in each fuel cycle. This information is cross-checked for consistency against operational records and initial fuel inventories.

The antineutrino detection based technique being investigated here has been described elsewhere [1]. It differs from the declaration and item accountancy methods described above in fundamental ways: first, the detector is under full control of the safeguards agency, and is thus distinct from the operator declarations of power and burnup, which depend on the good faith of the operator. Second, as opposed to item accountancy, it can provide independent, direct, real-time bulk accountancy of the fissile inventory from well outside the core, while the reactor is online. Third, it provides a direct, real-time measurement of the power of the reactor, which constrains fissile content. These independent measurements can be directly compared to declarations and used in conjunction with other IAEA accountancy and surveillance metrics.

We have demonstrated many of the important features of this technique, including unattended and continuous operation for long periods of time, non-intrusiveness, and sensitivity to reactor outages and power changes, using a device called “SONGS1” [2-5]. In this work, we describe the development of two new detectors that utilize different detection media. These new designs improve the ease with which such monitoring devices can be deployed at reactors, but make the task of identifying antineutrino interactions slightly more difficult.

2 Antineutrino Measurements of Interest for Reactor Safeguards

The antineutrino count rate and energy spectrum are both directly related to the reactor power and the fissile isotopic content of the core. As a reactor proceeds through its irradiation cycle, the mass and fission rates of each fissile isotope varies in time. Uranium and plutonium are both consumed by fission throughout the cycle, while the competing process of neutron capture on ^{238}U produces plutonium. The change in relative fission rates occurs even when constant power is maintained. This variation in turn causes a systematic shift in the antineutrino flux, known as the “burnup effect”. The effect has long been recognized and corrected for in reactor antineutrino physics experiments.
Antineutrino emission in nuclear reactors arises from the β-decay of neutron-rich fragments produced in heavy element fissions. In general, the average fission is followed by the production of about six antineutrinos that emerge from the core isotropically and for all practical purposes without attenuation. The average number of antineutrinos produced per fission is significantly different for the two major fissile elements ^{235}U and ^{239}Pu. Hence, as the core evolves and the relative fission fractions of ^{235}U and ^{239}Pu change, the antineutrino flux from the core will also change.
Using the ORIGEN/SCALE reactor simulation package [6], we have performed an assembly-level simulation of a PWR reactor core. The simulation package provides the mass and fission densities for each assembly in the core as a function of burn-up step. Using these simulated values in the formula

$$(1)\quad \frac{dN_{\bar{\nu}}}{dt} = k \cdot P \cdot \sum_i \frac{f_i}{E_i^f} \int dE_{\bar{\nu}} \cdot \sigma(E_{\bar{\nu}}) \frac{dN^i_{\bar{\nu}}}{dE \cdot fission}(E_{\bar{\nu}}) \ ,$$

we can predict the antineutrino rate from the reactor source as a function of time or burnup step. In the formula, k is a constant depending only on the detector mass and standoff distance, and P is the reactor thermal power. The defining relation for the isotope power fractions f_i is given by:

$$f_i = \frac{\frac{dN_i^{fission}}{dt} E_i^{fission}}{P} \ ,$$

where $\frac{dN_i^{fission}}{dt}$ is the fission rate and $E_i^{fission}$ the energy release per fission for the *i*th fissile isotope. The index *i* runs over the main fissioning isotopes: ^{235}U, ^{239}Pu, ^{241}Pu or ^{238}U.

$\frac{dN^i_{\bar{\nu}}}{dE \cdot fission}$ is the antineutrino energy density in units of events per MeV and fission, and $\boldsymbol{\sigma}(E_{\bar{\nu}})$ is the microscopic cross-section for the inverse beta decay process used to detect the antineutrino, depending on the antineutrino energy $E_{\bar{\nu}}$. $\boldsymbol{\varepsilon}(E_{\bar{\nu}})$ is an energy dependent detection efficiency, defined as the ratio of detected to interacting events in the target. In equation (1) the sum is over all fissioning isotopes, and the integral is over the antineutrino energy. The equation clearly shows the antineutrino rate dependence on both the reactor power P, and on the sum over fission rates. While not the subject of this article, we note that the energy spectrum of the antineutrinos can be further exploited to extract or constrain the individual isotopic masses throughout the cycle.

Figure 1 shows that the antineutrino rate changes by about 12% between refuelings. The same simulations allow us to predict the beginning and end of cycle fissile masses.

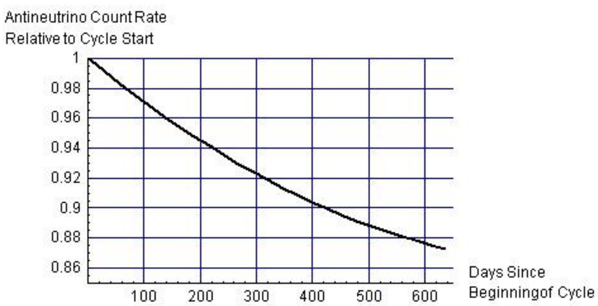

Figure 1: The predicted antineutrino count rate through a 637 day cycle, corresponding to the duration of SONGS Unit 2 reactor cycle 13. The rate is normalized to its value at beginning-of-cycle.

The current simulation marks an advance relative to our earlier simulations, since it includes specific densities on a per-assembly rather than core averaged basis. The input fuel isotopics for this simulation are taken from the San Onofre Nuclear Generating Station Final Safety Analysis Report [7]. This report provides a nominal fuel loading which differs by a few percent from the actual fuel load in recent cycles. The antineutrino rate curves shown in Fig. 1 will therefore differ – also by a few percent – from the actual results for the cycle covered by the current antineutrino data set. However, the approximate size of the burnup effect and the overall downward trend in the antineutrino rate are clearly revealed by the simulation.

3 Antineutrino detection through the inverse beta interaction

We use the (relatively) high probability inverse β-decay reaction

(2) $\boldsymbol{\bar{\nu} + p \rightarrow e^+ + n}$

Here the antineutrino ($\boldsymbol{\bar{\nu}}$) interacts with quasi-free protons (p) present in the detection material. The neutron (n) and positron (e+) are detected in close time coincidence, providing a dual signature that is robust with respect to the backgrounds that occur at the few MeV energies characteristic of these antineutrinos. The addition of Gadolinium (Gd) to the detection medium reduces the capture time of the neutron from about 200 μs to approximately 30μs, providing a much tighter time signature and commensurate reduction in uncorrelated background. Furthermore, neutron capture on Gd produces a shower of γ-rays with a total energy of close to 8 MeV, significantly higher than the 2.2 MeV γ-ray that results from the capture of neutrons on protons.

The signature of antineutrino interaction is thus a pair of relatively high energy events in a short time interval. Accidental coincidences from random neutron and gamma interactions, as well as correlated event pairs created by muogenic fast neutrons can also create antineutrino-like events. Modest overburden at the detector helps reduce the correlated backgrounds: a muon veto shield tags many of the surviving muons so that their associated backgrounds can be removed. Correlated backgrounds have the same time structure as the antineutrinos and are indistinguishable event-by event (in this detector) from antineutrinos. Therefore, these can only be measured during reactor outages, making the relatively rare outage periods (5% to 10% of the total cycle time) especially important for full determination of backgrounds in reactor-based antineutrino detectors.

4 The SONGS1 Detector

To allow comparison to the new designs, we describe here the essential features of the SONGS1 detector that operated at SONGS from late 2003 until 2007. SONGS1 is located in the tendon gallery of Unit 2, resulting in a core-detector separation of about 25 m. This gallery is an ideal location for the detector, since it is close to the core while remaining outside of the containment structure and away from daily reactor operations, and since it is about 20 m underground, providing an attenuating overburden for cosmic rays. The detector consists of three subsystems; a central detector containing the liquid scintillator target read out by photomultiplier tubes, a passive water or polyethylene shield on all sides, and a muon veto system placed outside the water shield on five sides of the detector.

• The Central Detector

The central detector, seen in Fig. 2, consists of two identical stainless steel cells, each with inner dimensions 17” by 17” by 40”. These are filled with 0.64 tons of Gd doped liquid scintillator. Scintillation light generated by the interaction of particles in the cells is converted to electrical signals by 9” PMTs (two per cell, not shown in figure).

• The Neutron/Gamma Shield

Gamma and neutron rates in the central detector are reduced by passive water or polyethylene shielding, which surrounds the detector on six sides. It is especially important to reduce the flux of neutrons impinging on the cells from outside the detector, as these can produce signals that mimic antineutrinos.

• The Muon Veto System

An approximately one inch thick plastic scintillator envelope identifies and rejects nearby cosmic rays and their associated interaction products. As shown in Fig. 2, the envelope is comprised of scintillator paddles of different sizes placed on five sides of the detector, readout by photomultiplier tubes.

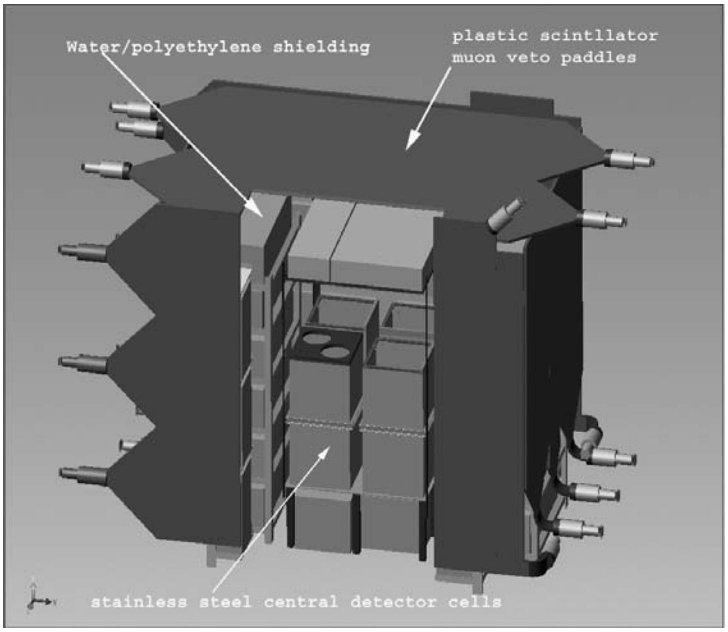

Figure 2. The SONGS1 detector. The central four stainless steel cells have an approximate cubic meter footprint. These are surrounded by water/polyethylene shields, and a five-sided muon veto system.

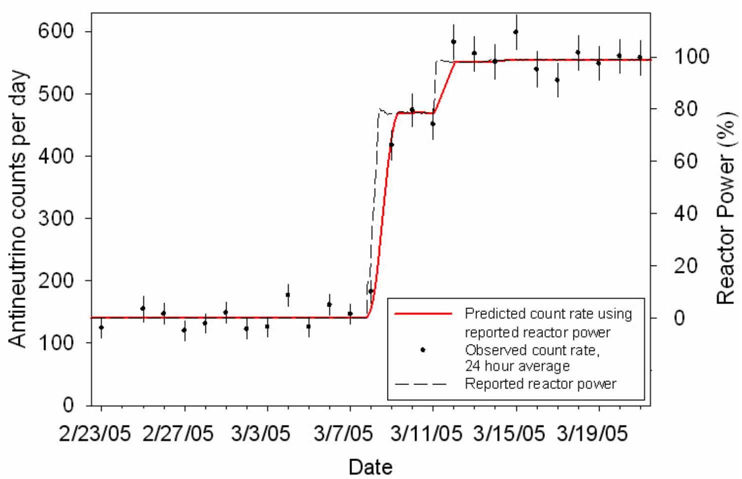

Figure 3 A 2005 transition from zero power to full power in SONGS Unit 2. An approximate three day period is shown in which the reactor was operated at 80% of full power. The antineutrino rate clearly tracks this power excursion.

As indicated in Fig.3, SONGS1 detects about 400 reactor antineutrinos per day when SONGS Unit 2 is at full power, a detection efficiency of about 10%. This design has been very successful, demonstrating unattended and continuous operation for long periods of time, non-intrusiveness, and sensitivity to reactor outages and power changes [2-5]. The primary disadvantage of SONGS1 is the use of a liquid scintillator. The scintillator used, Bicron BC525, is slightly flammable, with a relatively high flash point of 178^{o}F, and the total combustible inventory of the scintillator in the detector is about 55 million BTU. The use of a liquid medium requires special care to prevent any spillage or leakage and, in the current design, necessitates onsite assembly of the device.

5 Deployable Design #1: Solid Plastic Scintillator

To avoid the limitations of the liquid scintillator device, we have designed and deployed an antineutrino detector based upon a solid plastic scintillator (BC-408). It is important that we retain the neutron capture capability of the Gd doped liquid scintillator; in the plastic scintillator design this was achieved by interleaving Gd coated Mylar sheets between 2 cm thick slabs of plastic scintillator (Fig. 4).

The primary disadvantages of this approach are:

1. the BC-408 scintillator has 10% fewer protons (antineutrino targets) per cubic cm than the BC-525 liquid.
2. the introduction of dead material (Gd coated Mylar) into the active volume of the detector. This degrades the energy resolution of the detector, and reduces the antineutrino detection efficiency
3. a smaller fraction of neutrons generated in inverse beta reactions capture on Gd than in the BC-525 liquid (in BC-525 the ratio of captures on Gd vs H is 80%:20%, while in this design it is 60%:40%).

The primary advantages are:

1. the BC-408 plastic scintillator is non-flammable
2. the combustible inventory is reduced by about 25% for a given scintillator volume
3. the device can be preassembled offsite

One half of the SONGS1 liquid scintillator was replaced with an equivalent volume of plastic scintillator in 2007. The plastic scintillator detector is sensitive to neutron capture and correlations in much the same way as the liquid scintillator. As indicated in Fig. 5, it is also sensitive to reactor power changes.

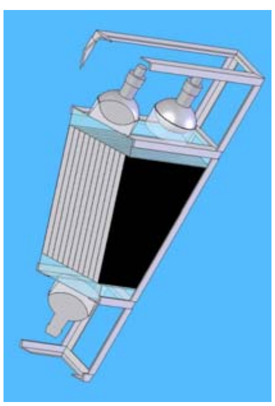

Figure 4. A cutaway view of the plastic scintillator design.

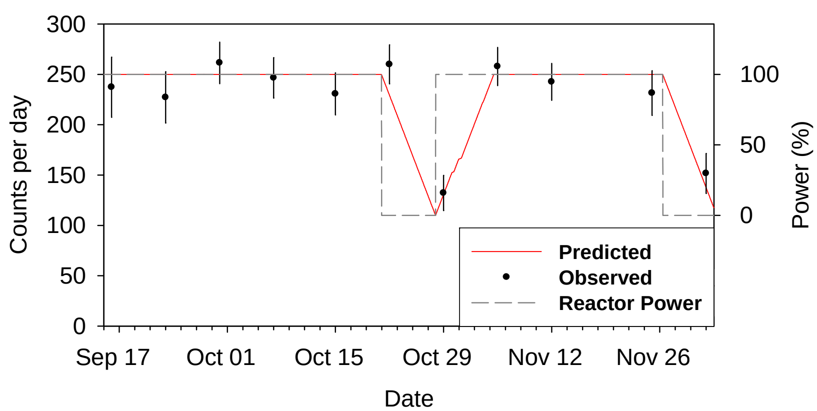

Figure 5. The response of the plastic scintillator design to two reactor outages. The device is clearly sensitive to reactor power changes.

5 Deployable Design #2: Water Cerenkov

Another approach that we have investigated is the use of Gd-doped water as a detection medium. Cerenkov light produced by charged inverse-beta reaction products would be detected using PMTs. This approach has been suggested for use in large neutrino physics detectors, and it has obvious benefits for this application. The water detection medium is:

1. completely non-flammable and non-combustible.
2. inexpensive and easy to handle
3. insensitive to the main *correlated* background that can mimic antineutrino interactions – recoil protons produced by cosmogenic fast neutrons

The primary disadvantage of this approach is the very low Cerenkov light yield (10s of photons per MeV, vs 1000s of photons per MeV for scintillator), which results in very poor energy resolution.

A 250 liter water tank, readout by 8 PMTs, (Fig. 6) was installed at SONGS in 2007. This tank was surrounded by a five sided muon veto, but had no other shielding. This device is clearly sensitive to neutron captures on Gd (Fig. 7) and neutron capture correlations from a fission neutron source. We are yet to observe a reactor antineutrino signal in this device, due to high background rates. We will soon deploy this water tank within the SONGS1 shielding, which should allow for a reactor antineutrino signal to be observed.

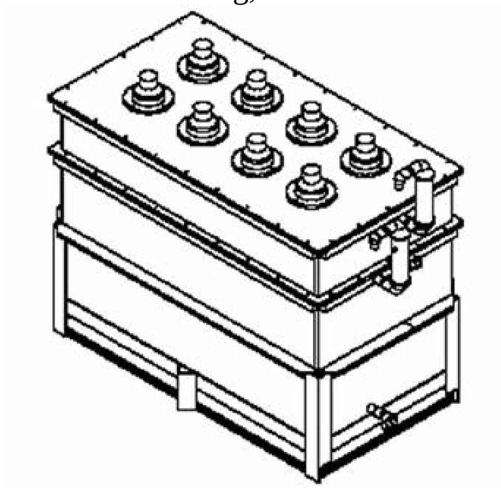

Figure 6. The 250 liter water tank that has been installed at SONGS. A main tank of purified Gd doped water is coupled to a smaller tank holding 8 PMTs.

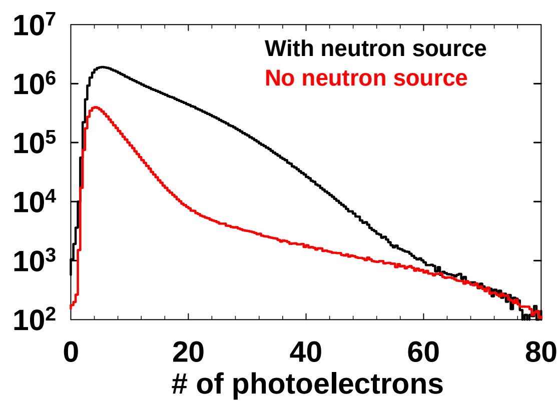

Figure 7. The response of the water Cerenkov detector to background and a neutron source. The device is clearly sensitive to neutron captures on Gd.

Conclusions

Our experimental campaign using SONGS1 detector has demonstrated many of the essential features of antineutrino detection that make it of potential interest for IAEA safeguards, including practical deployment of a simple and robust detector, unattended operation for months to years at a time, sensitivity to fissile content of the core, and real-time power monitoring capability. To extend the deployability of this monitoring technique we have investigated two alternate antineutrino detection technologies that reduce or eliminate the amount of combustible material used; one based upon plastic scintillator and the other on Gd doped water. The plastic scintillator design is clearly sensitive to reactor power changes; ongoing work is searching for sensitivity to reactor fuel evolution. We have yet to demonstrate antineutrino detection in the water Cerenkov detector, but this should be possible as the device is sensitive to neutron capture correlations from a fission neutron source. Data taking with the addition of passive shielding is planned to attempt to confirm this.

Acknowledgements

We continue to be grateful to the staff at the San Onofre Nuclear Generating Station for their generous assistance, which has made it possible for us to deploy and operate our detectors. We thank Georg Aigeldinger and Jim Brennan of SNL for their assistance constructing and deploying the Solid Plastic Scintillator detector.

References

[1] A. Bernstein, Y. Wang, G. Gratta, and T. West, *J. Appl. Phys.* **91** (2002) 4672.
[2] N.S. Bowden, et. al, First Results from a Nuclear Reactor Monitoring Antineutrino Detector, *Proceedings of the INMM 45th Annual meeting*, July 2004
[3] A. Bernstein, et. al, First Recent Results from a Test of Reactor Monitoring with a Cubic Meter Scale Antineutrino Detector, *Proceedings of the INMM 45th Annual meeting*, July 2006
[4] N.S. Bowden, et. al, Experimental results from an antineutrino detector for cooperative monitoring of nuclear reactors, *Nuclear Instruments and Methods in Physics Research A* 572 (2007) 985
[5] A. Bernstein, et. al, Monitoring the thermal power of nuclear reactors with a prototype cubic meter antineutrino detector, *Journal of Applied Physics* 103, 074905 (2008).
[6] I. C. Gauld, et. al., ORIGEN-ARP: Automatic Rapid Processing for Spent Fuel Depletion, Decay, and Source Term Analysis," ORNL/TM-2005/39 (2005)
[7] Final Safety Analysis Report: San Onofre Nuclear Generating Station Units 2 & 3, Southern California Edison Company and San Diego Gas & Electric Company.

LLNL-CONF-404568
This work was performed under the auspices of the U.S. Department of Energy by Lawrence Livermore National Laboratory in part under Contract W-7405-Eng-48 and in part under Contract DE-AC52-07NA27344.
Sandia is a multiprogram laboratory operated by Sandia Corporation, a Lockheed Martin Company, for the United States Department of Energy under contract DE-AC04-94AL85000